Optimization of Power-Cycle Arrangements for Supercritical Water Cooled Reactors (SCWRS)

L. Lizon-A-Lugrin[1], A. Teyssedou[1] and I. Pioro[2]
[1] Nuclear Engineering Institute, Engineering Physics Department,
École Polytechnique de Montréal, Montréal, Québec, Canada
[2] Faculty of Energy Systems and Nuclear Sciences,
University of Ontario Institute of Technology, Oshawa, Ontario, Canada

Abstract

An innovative optimization technique based on the use of "genetic algorithms" is used to analyze thermodynamic power cycles proposed for running future Supercritical Water Cooled Reactors. The front of Pareto generated by the proposed methodology shows that it is still possible to increase both the thermal efficiency and the mechanical power of proposed systems. In some cases, Pareto's landscapes show particular behaviors suggesting that the optimization can be achieved by modifying a limited number of decision variables. However, work is still required to implement simulations that are more realistic, i.e., including actual turbine design and operation conditions.

1. Introduction

The world energy demand is continuously rising due to the increase of both world population and standard quality of life. According to the International Agency of Energy, the world primary energy demand is expected to augment by up to 45% by 2030 [1]. It is obvious that present observed trends in energy supply and consumption do not satisfy environmental sustainability. Thus, to maintain an acceptable economy growth by ensuring appropriate social standards, new technologies of energy conversion must urgently be developed.

Within this framework, a Generation IV International Forum (GIF) was established by the participation of 10 countries to collaborate for developing nuclear power reactor that will replace the present technology by 2030. The principal characteristics of this new generation of nuclear reactors, among others are: economic competitiveness, sustainability, safety, reliability and resistance to proliferation. In order to meet these requirements, six nuclear power reactor concepts were selected by GIF members' [2]. Among these technologies, Canada has oriented its efforts towards the design of a Supercritical Water Reactor (SCWR). This system will use water at supercritical conditions as the principal coolant, running at about 625^{o}C and 25 MPa [3]. Thereby, the thermal efficiency of this kind of power plant will largely compete with actual supercritical steam power boilers. In addition, the high coolant temperature will enable not only the production of electricity, but also other energy applications (i.e., hydrogen production, sea water desalinisation, petroleum extraction, etc.) to be better achieved.

From a thermodynamic cycle viewpoint, the use of a supercritical fluid allows heat transfer without phase change to be obtained. Therefore, risks associated to the possibility of triggering critical heat flux conditions, in principle, are largely reduced or eliminated. Further, the use of steam generators and steam separators can be completely avoided in SCWR. In addition, it is also possible to use direct thermodynamic cycles where the supercritical fluid expands right away in the turbine without the necessity of using intermediate steam generators [4]. To this end, there are still great amount of work to be carried out to establish the most reliable and optimal cycle topology for this type of applications. Several steam-cycle arrangements used in existing thermal power plants have been extensively discussed among others by Naidin et al. [5]. In particular, the authors present a comparison of different thermodynamic cycles that could be appropriate to run Supercritical Water Nuclear Power Plants (SCWNPP). It must be pointed out, however, that none of the proposed cycles have been optimized yet. It is obvious that from an engineering viewpoint this constitutes a key issue. Thus, the present work is intended to fulfill this gap by including the optimization of different SCWNPP cycles by using genetic algorithms. To perform these calculations, models written in Matlab and an in house optimiser developed around evolutionary algorithms are applied [6-8].

2. Simulation and optimization strategy

The optimization of power plants constitutes multi-objective optimization problem where several objective functions must be satisfied simultaneously [7-9]. In most cases, the objectives conflict one with each other, which makes them unlikely to be satisfied by a single choice of controlling variables. Therefore, to achieve an optimal design, some trade-offs between objectives must be determined. Thus, a general formulation of a multi-objective optimization problem having n objective functions and m decision variables can be summarized (e.g., for a minimization case) as follows:

$$\begin{aligned} &\text{Minimize} \quad f_i(X) \qquad i = 1,2,...,n \\ &\text{Subjected to the constraints:} \\ &\qquad g_j(X) \geq 0 \qquad j = 1,2,...,p \end{aligned} \tag{1}$$

Where $X = (x_{1,} x_2, ..., x_n)$ is a vector, while $g_j(X)$ is a component of vector having p constraints. In general, there is no a single combination of decision variables x_n, which is able to simultaneously minimize all components of the vector $f_i(X)$. Therefore, the optimization will be represented by a set of trade-off solutions. To determine if a solution is in fact one of the best possible trade-offs, the "Pareto optimality" concept is used [10]. It permits a hierarchy among all solutions of a multi-objective optimization problem to be established. Thus, best solutions of the set are called "Pareto solutions" and they can be determined using multi-objective evolutionary algorithms [11]. To perform the present work, an efficient and robust evolutionary algorithm called "BEST" [9] is used. This methodology is able to tackle quite difficult multi-objective optimization problems without consuming awesome computational time. In fact we have developed the algorithm for treating complex, large-scale energy systems, where traditional methods are difficult to implement or are not able to work at all [12].

Unlike classical evolutionary algorithms that promote non-dominated solutions at each generation, the present approach consists of emphasizing dominated and non-dominated ones to drive the searching process towards the boundaries of the feasible region. To fulfill this requirement, a "C*orridor Header Evolution Tracking*" strategy is successfully implemented and used to treat power systems [7,9]. Solutions inside these corridors become parents for reproducing offspring in the next generation of a genetic algorithm [12,13]. Thus, an evolution process is applied to captured individuals that then undergo both crossover and mutation operations. The structure of the optimization algorithm is shown in Figure 1. In order to increase spreading of individuals and thus to fix more quickly the boundary of the feasible region, the probability of mutations is initially quite high (70% to 80%). Moreover, there is no special mechanism for the maintenance of the diversity because the corridor strategy implicitly fulfills this task [8]. In addition, the exploration of a promising area (i.e., contour of the feasible region) is achieved by using a crossover operator whose probability increases adaptively as mutations decrease.

The metric used to control mutations and crossovers is established by following the progression of the boundary formed by individuals in the corridors, calculated with the following equation:

$$d = \sum_{j=1}^{N} \left[\frac{1}{C} \sqrt{\sum_{i=1}^{C} \left(\frac{f_{j,i}^{t} - f_{j,i}^{t-1}}{f_{\max} - f_{\min}} \right)^2} \right]. \quad (2)$$

In this equation, $f_{j,i}^{t}$ represents the evaluation of objective j of an individual inside the corridor i at generation t; $f_{\min}$ and $f_{\max}$ are the lower and upper bounds of the objective j; N is the number of objectives and C is the number of corridors.

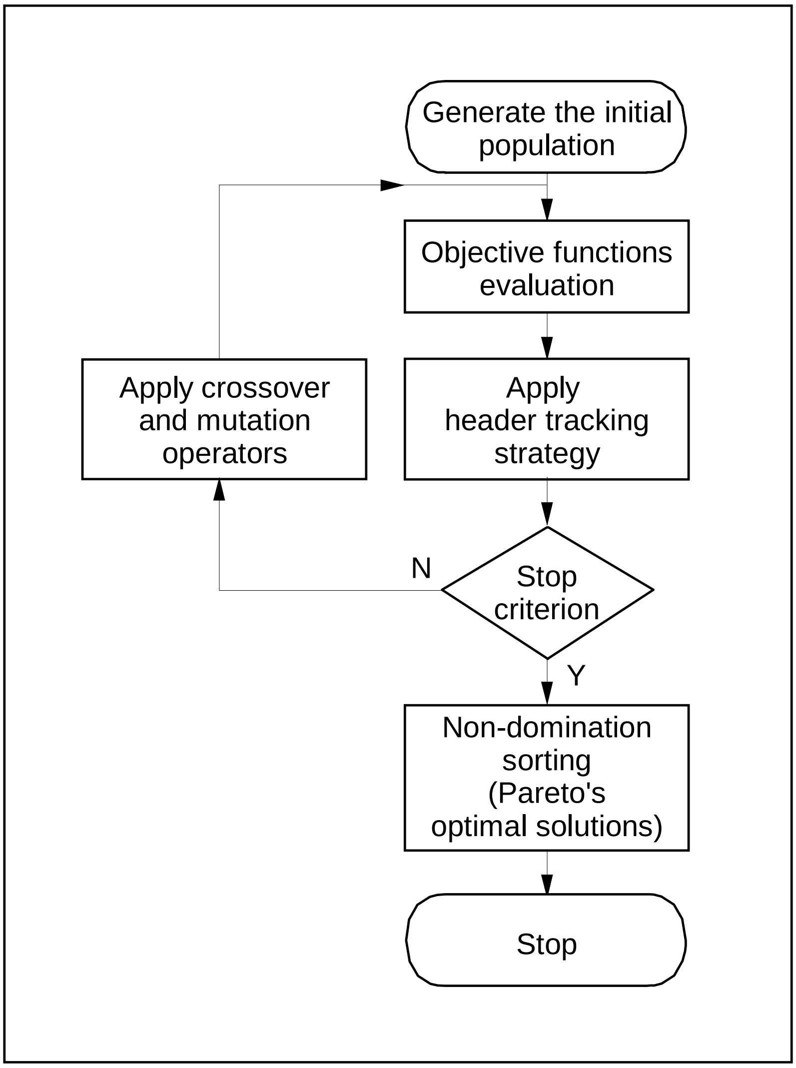

Figure 1. Flow sheet of the proposed algorithm.

The value obtained from Equation (2) is then used to determine a "*control*" parameter calculated as: $control = \ln(d)$. After multiple trials, a triggering between operations was established based on this parameter and the best values are suggested in Table 1. The solution searching process is based on the strategy given in Herrera et al. [14]. The probabilities used for each operator during the present work are summarized in Table 2. As the population converges towards the contour of the feasible region, it is apparent that parameter d decreases, which allows a convenient limit at which the algorithm stops the searching process, to be introduced. Finally, a non-domination sorting procedure is executed to determine Pareto's optimal solutions.

Table 1. Suggested values for the *control* parameter.

Trigger or action	*control* parameter
Exploration triggering	$control \geq -8$
Hybrid triggering	$-12 \leq control \leq -8$
Exploitation triggering	$-18 \leq control \leq -12$
Stop process	$control \leq -18$

Table 2. Summary of searching process operators.

Searching phase	Operator	Probability (%)	Type
Exploration	Mutation	90	Random
	Crossover	10	Uniform
Hybrid	Mutation	10	Probabilistic
	Crossover	90	Simulated binary
Exploitation	Mutation	10	Probabilistic
	Crossover	90	Arithmetic

To handle thermodynamic power-cycles, the optimization technique is coupled to appropriate power plant thermodynamic models that are discussed in more detail in Section 4. Figure 2 represents the framework implemented to perform both plant simulations and optimization.

The strategy is composed of the optimizer and a power plant simulator based on specific plant thermodynamic models. The two modules communicate to each other by exchanging data from two blocks. To this aim, a “Dynamic Data Exchange” (DDE) protocol running under the Windows XP environment is implemented. The first block converts the data into physical variables that are sent to the simulator, while the second one evaluates objectives and constraints imposed to the problem, by using the results from the simulations. The optimizer generates an initial random population of solutions or individuals. They are then used by the plant simulation module to evaluate thermodynamic states that are invoked to calculate objectives and constraints required to run, once again, the optimizer. Based on the fitness of the individuals, the best ones are selected to pass crossover and mutation operators and thus, to reproduce a new population that should be more efficient than the initial one. This new population seeds the simulator and the process continues until a convenient stop criterion is reached.

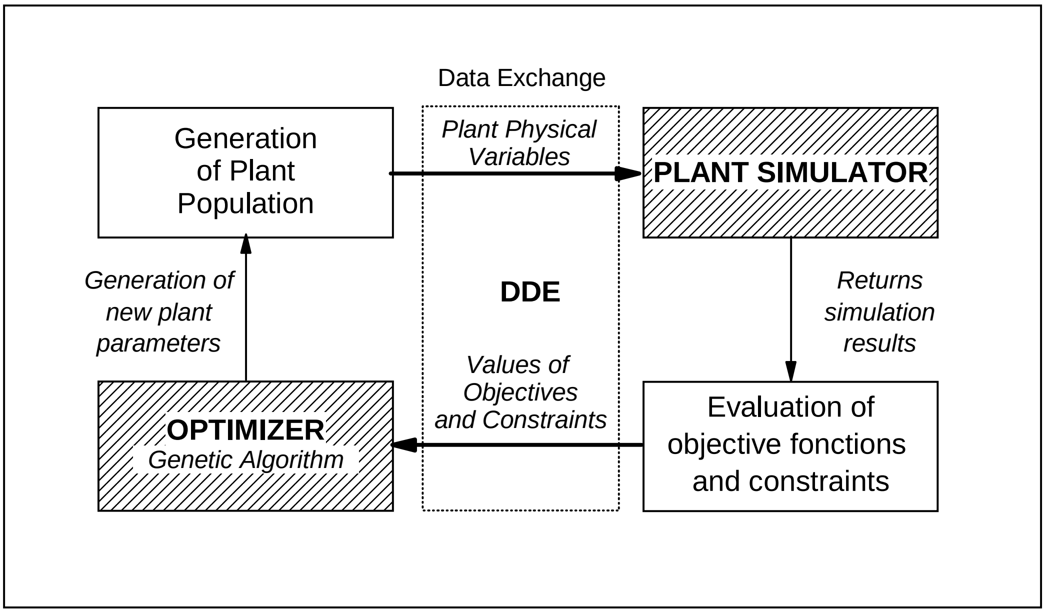

Figure 2. Optimization procedure framework.

The proposed methodology has been largely validated. In fact, the same optimization scheme has been used in conjunction with appropriate models to optimize cogeneration and advanced steam power plants [7-9]. In addition, a thermodynamic model quite similar to that used in this work was also applied to simulate the Gentilly-2 nuclear power plant. These calculations, which include models for major thermal equipments, were able to reproduce very closely actual operation conditions of the nuclear power station [15].

3. SCW cycle configurations

In this paper, four simplified thermodynamic cycles given in Naidin et al. [5] are optimized by using the methodology described in the former section. These power-cycles, summarized in Figures 3a to 3d , are proposed as the most suitable to be implemented in next generation of SCWNPP. Operation conditions taken from the same reference correspond to topologies that are variants of Rankine's type cycles working under the same supercritical water flow conditions of 25 MPa and 625°C performing the same mechanical work of 1200 MW. In addition, Figures 3c and 3d show two regenerative Rankine cycles which permit the thermal efficiency to be increased by using the latent heat of a fraction of steam extracted from the turbines to reheat the feedwater before it enters into the reactor core. It must be pointed out that the fractions of extracted fluid do not produce useful work but they allow the overall efficiency to be increased. Therefore, in such cases, the optimization clearly corresponds to a compromise between efficiency and mechanical work. In addition, the use of closed feedwater reheaters with two circulation pumps makes these systems more suitable for applications in SCWNPP. In fact, they can permit using less sophisticated pumps while tube-shell heat exchangers may better support the extremely high pressures that will be encountered in SCWNPP systems.

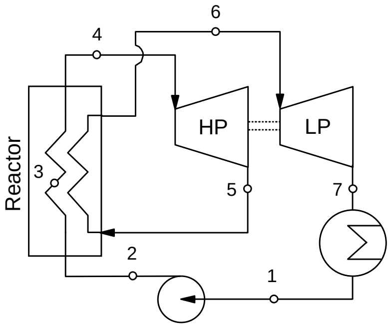

State	$T(^oC)$	$P(MPa)$	$h(kJ/kg)$
1	38.3	0.00677	160.8
2	39.1	25.0	186.0
3	350.0	25.0	1624.0
4	625.0	25.0	3567.0
5	345.0	4.9	3060.0
6	625.0	4.9	3725.0
7	38.3	0.00677	2275.0
Efficiency (%)			48.1
Mass flow rate (kg/s)			613.0

(a)

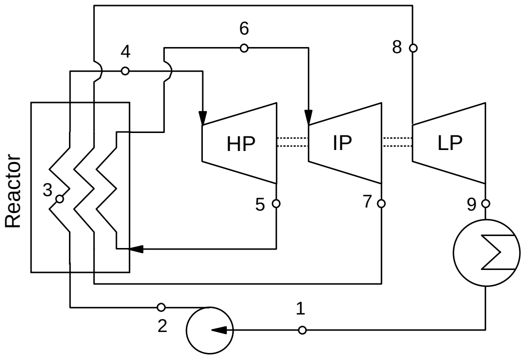

State	$T(^oC)$	$P(MPa)$	$h(kJ/kg)$
1	38.3	0.00677	160.8
2	39.1	25.0	186.0
3	350.0	25.0	1624.0
4	625.0	25.0	3567.0
5	410.0	7.6	3180.0
6	625.0	7.6	3705.0
7	418.0	2.3	3280.0
8	625.0	2.3	3745.0
9	38.3	0.00677	2390.0
Efficiency (%)			49.3
Mass flow rate (kg/s)			554.0

(b)

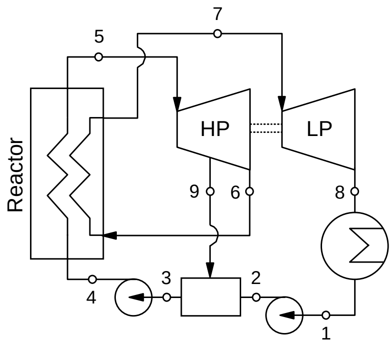

State	$T(^oC)$	$P(MPa)$	$h(kJ/kg)$
1	38.3	0.00677	160.8
2	38.8	14.9	175.0
3	340.0	14.9	1605.0
4	350.0	25.0	1624.0
5	625.0	25.0	3567.0
6	345.0	4.9	3060.0
7	625.0	4.9	3725.0
8	38.3	0.00677	2275.0
9	525.0	14.9	3385.0
Efficiency (%)			49.9
Mass flow rate (kg/s)			1030.0

(c)

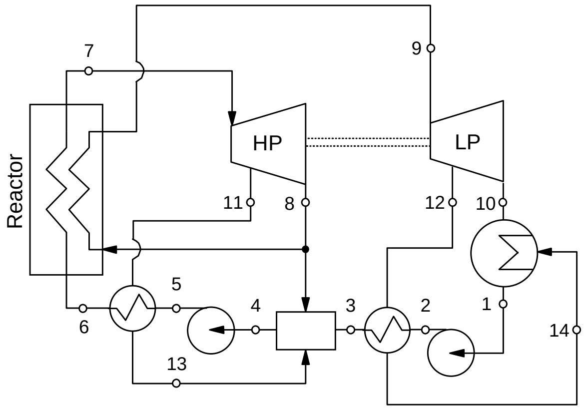

State	$T(^oC)$	$P(MPa)$	$h(kJ/kg)$	State	$T(^oC)$	$P(MPa)$	$h(kJ/kg)$
1	38.3	0.00677	160.8	8	350.0	5.0	3065.0
2	38.5	5.0	166.0	9	625.0	5.0	3725.0
3	200.0	5.0	850.0	10	38.3	0.00677	2270.0
4	265.0	5.0	1155.0	11	540.0	16.2	3415.0
5	270.0	25.0	1180.0	12	450.0	1.6	3314.0
6	350.0	25.0	1624.0	13	275.0	16.2	1210.0
7	625.0	25.0	3567.0	14	45.0	1.6	185.0
			Efficiency (%)	52.7			
			Mass flow rate (kg/s)	937.0			

(d)

Figure 3a-d. SCWNPP simplified thermodynamic cycles [5].

4. Plant simulation modelling approach

As shown in Figure 2, the optimization relies on a large number of plant simulations performed by changing randomly several key thermodynamic variables. Therefore, models for each cycle shown in Figures 3a-d are written in Matlab (version R2008a) [16]. The thermodynamic properties of water and steam are determined with the XSteam library [17] based on relationships given in IAPWS-97 [18]. For a wide range of temperature and pressures covering the supercritical region, both enthalpies and entropies calculated with this library are validated against similar values given in the water-steam table of Schmidt [19]. Relative differences, defined with respect to this table are partially compared in Figure 4. In general, it is observed that the XSteam library implemented in Matlab systematically underestimate (slightly) both enthalpies and entropies, however, maximum differences of about 1% occur within a limited region characterized by temperatures ranging from 375 to 385^{o}C.

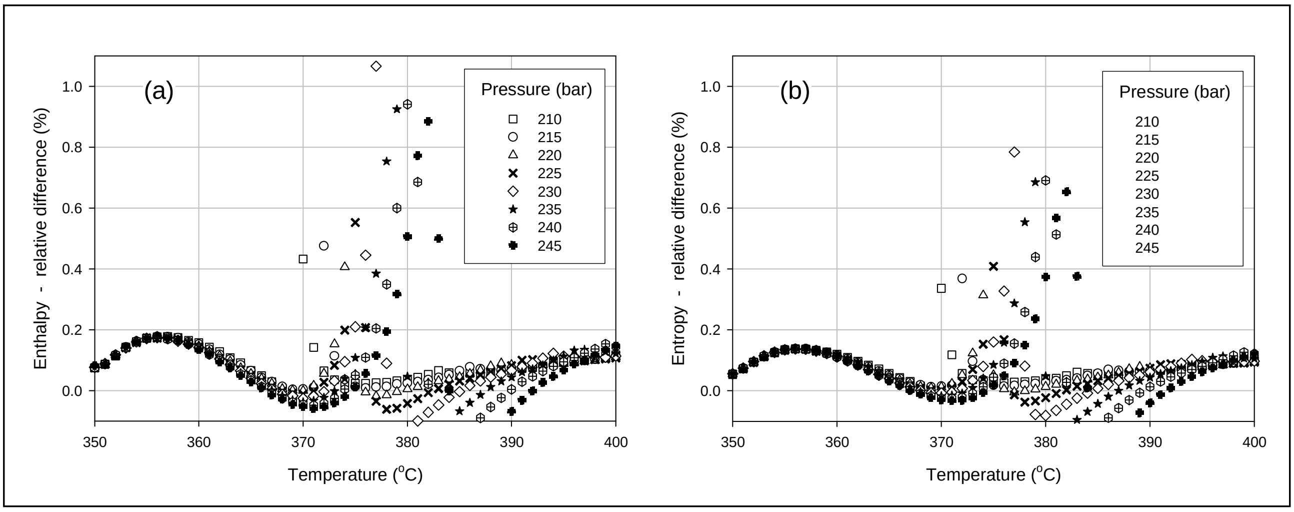

Figure 4. Comparison of water-steam properties predicted by XSteam [17] with values given in Schmidt [19] (a) Relative enthalpy difference; (b) Relative entropy difference.

In addition, to correctly compare both the thermal-cycle efficiency and the mechanical power obtained from the present optimization with those given in reference [5] we use the same assumptions and definitions. Therefore, equipments are considered adiabatic (i.e., ideal thermally insulated heat exchangers) and pressure losses in the heat exchangers and in steam extraction lines are neglected. Further, turbine groups and pumps are assumed to operate under ideally isentropic conditions. The calculation of cycle efficiency and mechanical power are estimated from the following objective equations:

$$\dot{W} = \dot{Q}_{in} - \dot{Q}_{out} \text{ and } \eta_{th} = \frac{\dot{W}}{\dot{Q}_{in}} , \tag{3}$$

where $\dot{W}$ represents the total mechanical power instead of the net one. Even though this definition of efficiency differs from the most common form, i.e., it does not include the mechanical power of the pumps, the amount of the power consumed by the pumps is usually very low compared to the output of the turbines, therefore, this effect is in general insignificant.

4.1 The turbine

Since the early 1950s the principal objectives in designing steam turbines consisted of increasing their performance (i.e., decrease internal irreversibilities) by achieving appropriate inter-stage pressure gradients by minimizing undesirable flow leakages and optimizing local velocity distributions [20]. From supercritical water viewpoint applications, first works were carried out in USA around the same epoch and then the technology spread out in Russia around 1960s. Utilities incorporated a commercial supercritical turbine technology in the USA with the construction of the AEP Philo unit 6, 125-MW power plant in 1957. The operating conditions of this systems are 31 MPa, 621/565/538°C [21]. Even though common supercritical water parameters used in state of the art fossil-fuelled power plant are 25 MPa and 600°C, few power plants also operate at higher pressure and temperature conditions (i.e., 31 MPa and 650°C). Most of these plants directly run supercritical turbines with capacities ranging from 300 MW to 1200 MW [3]. Modern supercritical turbines substantially differ from one manufacturer to another. Some of these differences concern turbine types (impulse or reaction), shaft combinations (cross compound or tandem), and the range of operating conditions (temperature, reheat pressure, etc.). The technology, however is improving continuously; thus, it is expected that in the near future they would be further developed for application in SCWNPP's. As mentioned above, and to compare the present results with those given in Naidin et al. [5], in this work the turbines are assumed isentropic. Figure 5 summarizes the modeling approach used to simulate the systems presented in Figures 3a-d. Thus, the mechanical power produced by the turbine is calculated as:

$$\left|\dot{W}_T\right| = \dot{m}\left[\left(h_o - h_1\right) + \sum_{i=1}^{n-1}\left(1 - \sum_{k=1}^{i} y_k\right)\left(h_i - h_{i+1}\right)\right]. \quad (4)$$

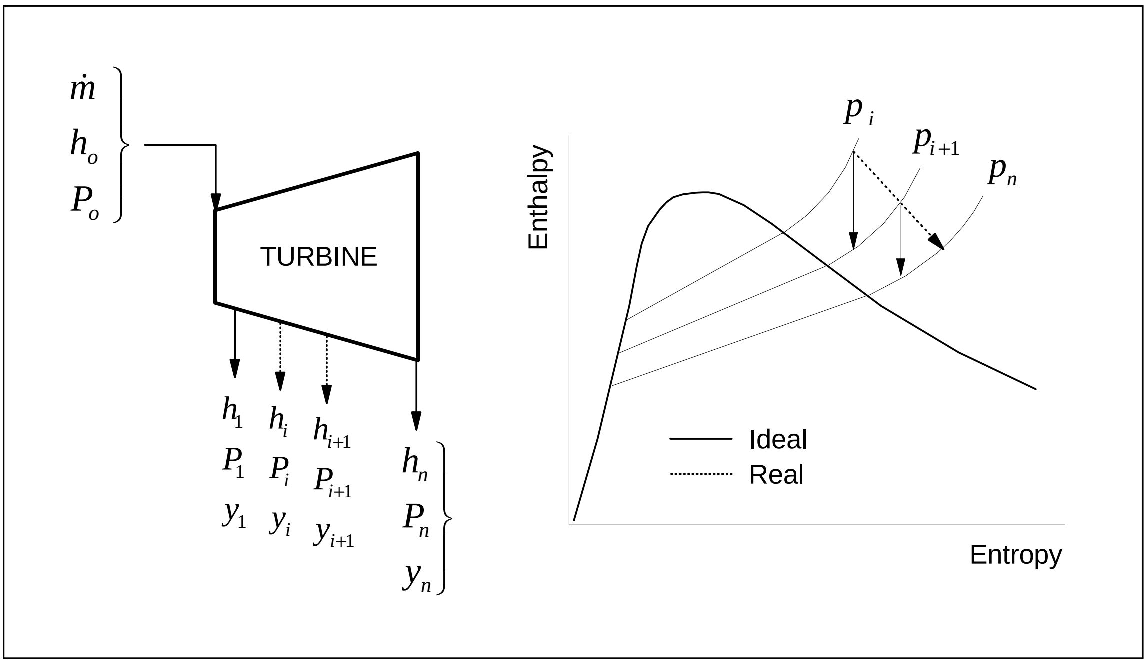

Figure 5. Simple modelling of multistage turbine groups.

4.2 The condenser

For all cycle studied, it is supposed that the condenser operates under a constant pressure of 6.77 kPa (Figures 3) which corresponds to a saturation temperature of 38.3°C. Similar to Naidin et al. [5], we assume that the condensate leaves the condenser as saturated liquid. Figure 6 shows the condenser modelling approach.

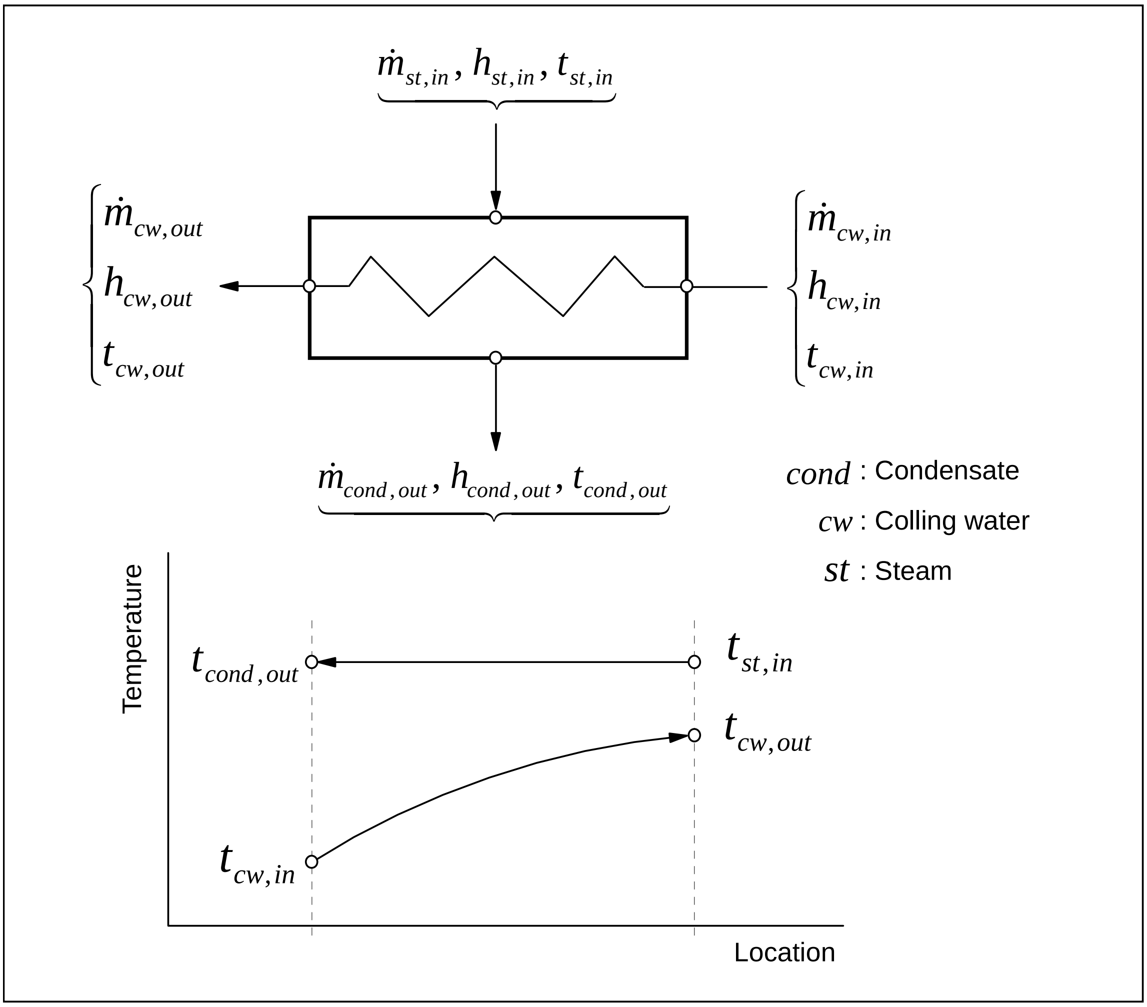

Figure 6. Simplified condenser model.

Following Figure 6, the energy balance equations are written as:

$$\begin{gathered}\dot{Q}_{cond} = \dot{m}_{st,in} h_{st,in} - \dot{m}_{cond,out} h_{cond,out} = \dot{m}_{cw,out} h_{cw,out} - \dot{m}_{cw,in} h_{cw,in} \\ \dot{Q}_{cond} = \dot{m}_{st}\left(h_{st,in} - h_{st,out}\right) = \dot{m}_{cw}\left(h_{cw,out} - h_{cw,in}\right) \\ \dot{Q}_{cond} = \dot{m}_{cw} C_p \left(t_{cw,out} - t_{cw,in}\right)\end{gathered} \quad , \tag{5}$$

where $\dot{m}_{st}$ and $\dot{m}_{cw}$ are the steam and cooling water mass flow rates respectively, and C_p is the water specific heat capacity determined at the mean cooling water temperature $= \left(\frac{t_{cw,out} + t_{cw,in}}{2} \right)$.

4.3 Feed water heaters

A considerable improvement in efficiency is obtained by reheating the feedwater before it enters into the reactor core (i.e., regeneration cycles). This process is commonly achieved by extracting some fractions of steam from various turbine stages and to regenerate the latent heat inside feedwater heat exchangers. Mainly two types of feedwater heaters are encountered in the power industry; direct contact or open type heat exchangers and tube-shell or closed type heat exchangers [22]. In open type feedwater heaters the extracted steam mixes with the water. They usually operate in such ways that permit both reheating the circulating fluid and extracting non-condensable gases prevailing in the system to be simultaneously obtained. Therefore, at the outlet of these units the water is usually under saturated liquid state. It is obvious that the simulation of this kind of reheaters is quite simple; they only require solving two equations (i.e., a mass balance and an energy balance) under constant pressure conditions. Since in this work pressure losses in the steam extraction lines are neglected, this pressure is directly controlled by the pressure prevailing at the extractions. It must be pointed out that to perform the optimization process, extractions are randomly changed; thus, their pressures also change. In shell-tube type feedwater heaters, however, heat is transferred from the steam to the water without contact between currents of fluids. Furthermore, since steam condenses inside the shell, the heat capacities, the temperature profiles and the heat transfer coefficients change along the whole process. Therefore, the simulation of this type of units requires an iterative procedure. In the present work we assume that the heat exchanger can be divided in the following three zones: *i*) superheating, *ii*) condensing and *iii*) drain-cooling, as shown in Figure 7. Because neither the geometrical nor the mechanical parameters of the heat exchanger are taken into account, the calculation scheme is relatively simple.

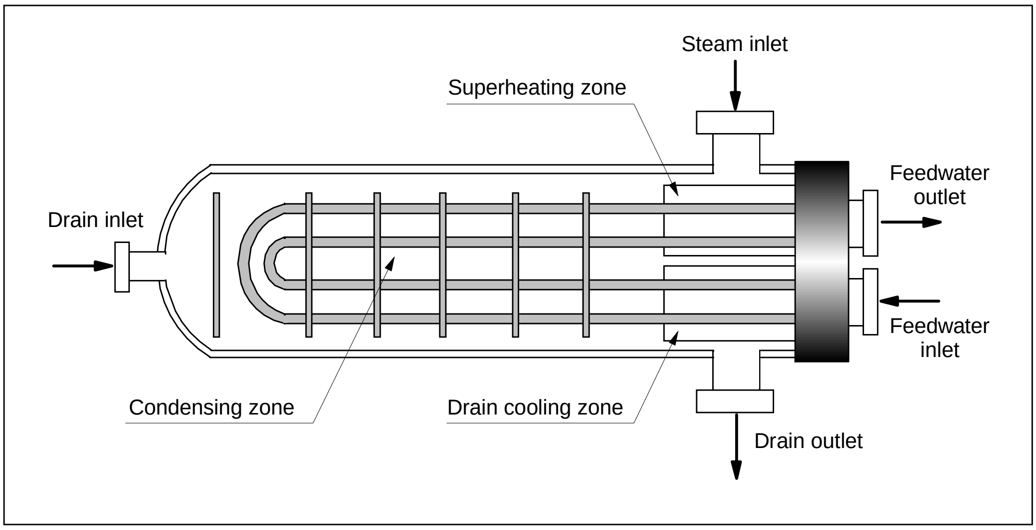

Figure 7. Typical three-zone feedwater heater.

Figure 8 shows expected temperature distributions as well as the variables used to simulate this type of feedwater reheaters.

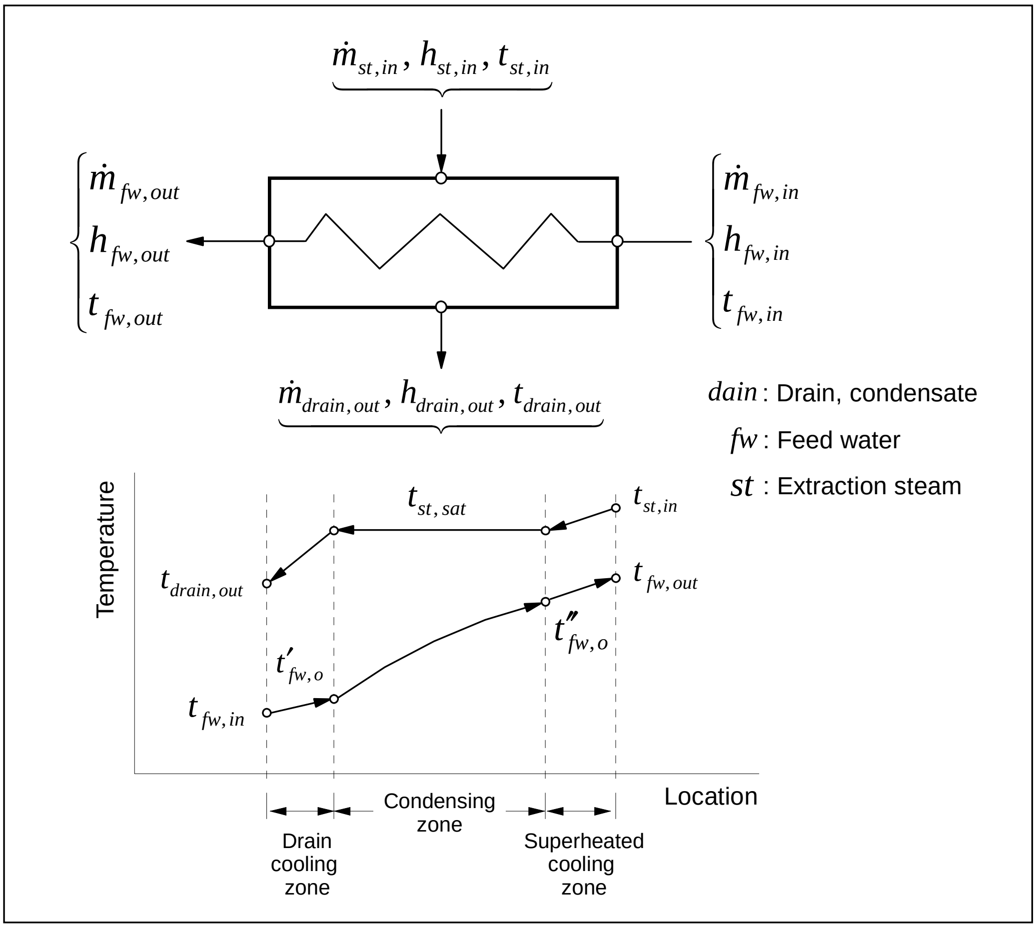

Figure 8. Flow diagram and temperature profiles of a three-zone feedwater heater.

4.4 Pumps

As mentioned before, pumps are considered isentropic; thus, their consumptions are calculated based on simple thermodynamic concepts. In all the cases these calculations are performed using the specific volume of the fluid determined at the inlet side. In turn, to avoid cavitation, inlet subcooling conditions are imposed as constraints.

5. Results of the optimization

The optimization strategy discussed in Section 2 jointly with the modelling approach described above is applied to each of the supercritical-water power cycles shown in Figure 3. All the optimizations are carried out by running the algorithm under the same conditions (see Figures 1 and 2). Thus, a constant population of individuals (=200), with the same number of generation (=100) and corridors (=60) are used. Previous trials have shown that these values are not very critical; thus they are arbitrary selected. It is obvious; however, that the computational time increases with increasing any of these quantities. Furthermore, the initial population of 200 solutions (i.e., individuals) required to run the genetic algorithm is generated by the thermodynamic model, where key thermodynamic variables (control parameters) are randomly changed. Depending on the type of cycle, these variables can be different. For instance for the simplest case shown in Figure 3a, only the pressures at states 5 and 6 are considered. Instead, for the complex case (Figure 3d) both pressures and extractions constitutes the control variables of the problem. In addition, the optimization must simultaneously satisfy the objectives (Equation 3) and the several constraints that are specific to each case. The Pareto's front obtained for the simplest cycle given in Figure 3a is shown in Figure 9.

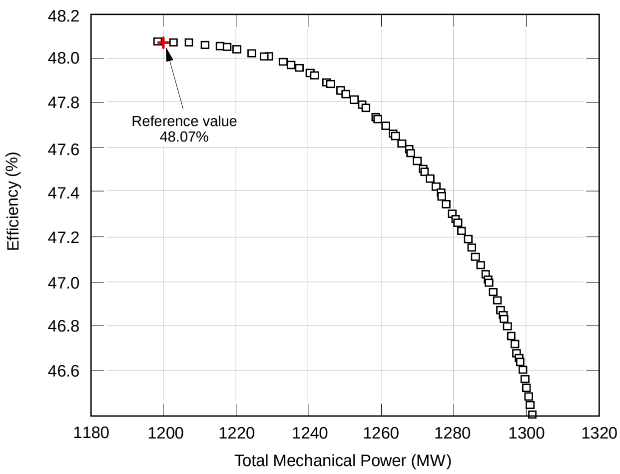

Variables	*Min.*	*Max.*
Pressures at 5 and 6 (*MPa*)	0.5	10
Constraints		
Steam quality	$x_1 = 0$	
Genetic Algorithm		
Population	200	
Max. generations	100	
Number of corridors	60	
Optimization Results		
Pressures at 5 and 6 (*MPa*)	0.5	4.985
Efficiency (%)	46.4	48.1
Mechanical power (MW)	1198	1301

Figure 9. Pareto's front obtained for the system shown in Figure 3a.

This figure includes a table that contains key values of the optimization. As can be observed the efficiency and mechanical power given in [5] are within the predicted Pareto's landscape. However, the present optimization results indicate that there exist other operation conditions that produce higher mechanical power at the cost of decreasing the overall efficiency. It is interesting to note that the efficiency given in the reference corresponds to almost the maximum output power that this plant can produce. For a double-reheat cycle (Figure 3b) the optimization variables are the pressures at the exit of the HP and IP turbines with a single constraint imposed to the quality at the inlet of the pump. Similarly to the former case the objectives are given by Equation 3. Pareto's front obtained for this case is compared with reference values in Figure 10. It is interesting to observe that in this case both efficiency and mechanical power given in reference [5] are much lower than the optimal conditions predicted by using the present methodology. Nevertheless, Pareto's front clearly shows the competition between the objectives (Equation 3) that is, efficiency decreases with increasing mechanical power and vice-versa. Note that in general the variations in discharge pressures permit better trade-offs to be achieved. It must be pointed out, however, that these changes must be validated against real operation conditions of the turbines. Therefore, the final optimization is not necessarily useful without introducing a tight interaction with plant design engineers. The single-reheat cycle with heat regeneration through an open type feedwater heater shown in Figure 3c, is optimized by changing the pressures at the extraction and at the exit of the HP turbine as well as the fraction of extracted steam. Equation 3 is used as objectives while at least three constraints must be satisfied during the process. Beside the restrictions imposed to some steam qualities, to avoid cavitation the liquid entering into the pump is forced to be slightly sub-cooled. The results of the optimization presented in Figure 11, show particular features. In fact, Pareto's front is characterised by three distinct zones. The analysis of this behaviour is quite complex. As a matter of fact, the representation given in Figure 11 corresponds to a simple projection of a multi-dimensional space into two dimensions (i.e., in this case this space has at least five dimensions). Therefore, only a careful representation of all variables that control the solution space can help us to understand the particular behaviour of Pareto's front. In some cases there are preponderate variables that determine the dynamics of the system.

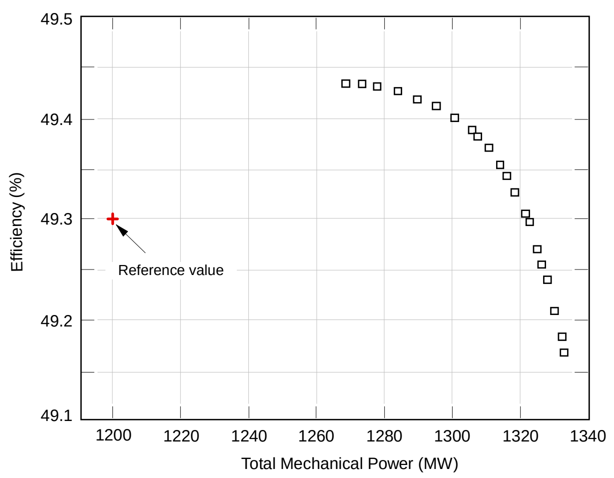

Variables	*Min.*	*Max.*
Pressures at 5 and 6 (*MPa*)	4	10
Pressures at 7 and 8 (*MPa*)	0.4	4
Constraints		
Steam quality	$x_1 = 0$	
Genetic Algorithm		
Population	200	
Max. generations	100	
Number of corridors	60	
Optimization Results		
Pressures at 5 and 6 (*MPa*)	4	5.6
Pressures at 7 and 8 (*MPa*)	0.4	1.05
Efficiency (%)	49.2	49.4
Mechanical power (MW)	1269	1333

Figure 10. Pareto's front obtained for the system shown in Figure 3b.

In this particular case we have observed that the first zone (Figure 11) seems to be controlled by the pressure in such a way that the efficiency decreases and the mechanical power increases with decreasing the pressure at the extraction and at the exit of the turbine.

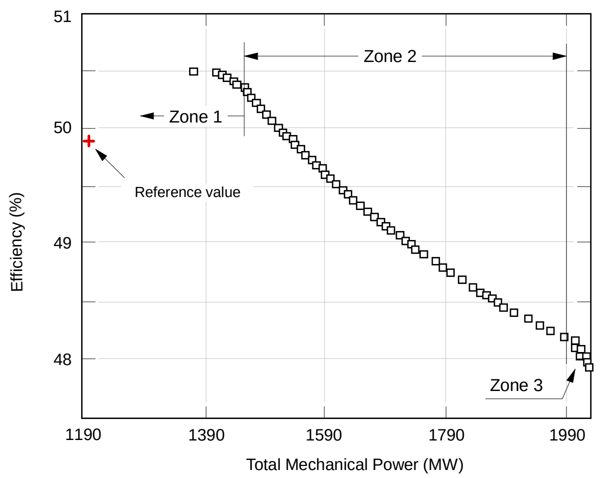

Variables	*Min.*	*Max.*
Pressures at 3, 2 and 9 (*MPa*)	6	20
Pressures at 6 and 7 (*MPa*)	2	6
Steam extractions *y* (%)	0.05	6
Constraints		
Steam quality	$x_1 = 0$	
Steam quality	$x_3 = 0$	
Enthalpy diff.	$h_{f3} - h_3 \geq 0$	
Optimization Results		
Pressures at 2, 3 and 9 (*MPa*)	8	9.6
Pressures at 6 and 7 (*MPa*)	2	3.6
Steam extractions *y* (%)	0.05	4
Efficiency (%)	47.9	50.5
Mechanical power (MW)	1374	2028

Figure 11. Pareto's front obtained for the system shown in Figure 3c.

The second zone seems to be controlled by the fraction of extracted steam; thus, efficiency decreases and mechanical power increases with decreasing the extraction mass flow rate. Finally, zone 3 appears to be mainly controlled by the pressure in a similar way as zone 1. Furthermore, it is interesting to note that Pareto's front provides a large number of possible solutions which permit higher efficiencies and mechanical work than those given in the reference, to be achieved. The regeneration cycle shown in Figure 3d is optimized by considering a larger number of degrees of freedom. Its optimization is based on pressures at the extractions and at the exit of the HP-turbine as well as steam fractions at points 11 and 12. Note that the fraction of steam from point 8 is imposed by the balance of mass and energy applied to the open reheater that works as the deaerator unit of the power plant. Therefore, the flow at the exit of this equipment is considered to be under saturated liquid condition, which is considered as an additional constraint of the problem. To avoid cavitation, subcooled conditions are also imposed to the liquid at the inlet of the pumps. Control variables and constraints are summarized in Figure 12. This figure also presents the Pareto's front obtained for this system as well as the reference plant state [5]. The front is characterized by four distinct zones. Even though all control parameters vary randomly along the front, each zone seems to be essentially conditioned by one preponderate variable. Hence, careful analyses of the predicted data (i.e., eight dimensions space) show that the first zone is mostly determined by the pressure at the exit of the LP-turbine (point 8 in Figure 3d). In this zone, efficiency decreases and mechanical power increases with decreasing the pressure. The second zone is mainly controlled by the fraction of steam extracted at point 11. It is observed that efficiency increases and mechanical power decreases with increasing the mass flow rate of this extraction. This result corroborates basic thermodynamic principles, i.e., the extraction of a fraction of steam allows a gain in efficiency at the expense of losing some turbines' work. The abrupt knee change observed in zone 3 of Figure 12 seems to be mostly controlled by the steam extracted at point 12; thus, thermal efficiency increases and the mechanical power decreases with increasing the extraction mass flow rate. Finally the last region is conditioned by the pressure at point 8 following behaviour similar to zone 1. It must be pointed out that the pressure at point 11 and 12 do not considerably change; they stay almost constant to their lowest limit imposed by the optimizer, therefore they do not have a significant effect on Pareto's front.

Similarly to other cases studied, the present optimization method provides a wide range of thermodynamic conditions under which both thermal efficiency and mechanical power are much higher than the values suggested in Naidin et al. [5].

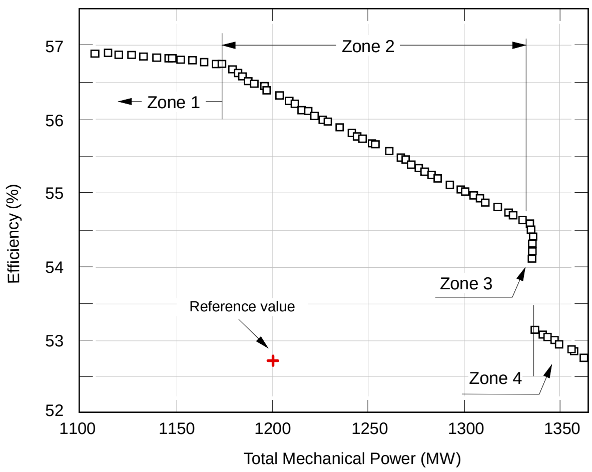

Variables	Min	Max
Pressure 11 (MPa)	12.15	20.25
Pressure 8 (MPa)	3.75	6.25
Pressure 12 (MPa)	1.2	2
Temperature 6 (C)	270	370
Extraction 11 x (%)	15	25
Extraction 12 z(%)	10	20

Constraints

Temperatures

$$|t_6 - t_8| \le 30^oC \qquad t_{11} - t_6 \ge 0 \qquad t_{12} - t_{13} \ge 0$$

$$t_{13} = t_5 + 6^oC \qquad t_{14} = t_2 + 6^oC \qquad t_{sat14} - t_{14} \ge 0$$

$$t_{sat13} - t_{13} \ge 0$$

Steam qualities

$$x_1 = 0 \qquad x_4 = 0$$

$$x_{10} \ge 0.85 \qquad x_{12} = 1$$

Extractions $x + y + z \le 60\%$

Figure 12. Pareto's front obtained for the system shown in Figure 3d.

Due to the relative complexity of this cycle, a comparison between the optimum conditions selected from the Pareto's front close enough to the reference case is given in Table 3. In general, the values of most thermodynamic variables are quite similar, however, major differences are observed around steam extractions. Thus, the total mass flow rate of steam extractions for the optimized system is about 11% higher than the reference case. However, it is interested to note that a higher total value of the extractions permits both thermal efficiency and mechanical power to be considerable higher than the reference case.

Table 3. Comparison between the reference case [5] and optimized system of Figure 3d.

	Reference case			***Present optimization***		
State	$T(^oC)$	$P(MPa)$	$h(kJ/kg)$	$T(^oC)$	$P(MPa)$	$h(kJ/kg)$
1	38.3	0.00677	160.8	38.4	0.00677	160.77
2	38.5	5.0	166.0	38.51	4.15	164.94
3	200.0	5.0	850.0	210.3	4.15	899.86
4	265.0	5.0	1155.0	252.53	4.15	1098.11
5	270.0	25.0	1180.0	257.93	25.0	1124.11
6	350.0	25.0	1624.0	351.99	25.0	1637.94
7	625.0	25.0	3567.0	625.0	25.0	3566.77
8	350.0	5.0	3065.0	322.57	4.15	3018.78
9	625.0	5.0	3725.0	625.0	4.15	3731.29
10	38.3	0.00677	2270.0	38.38	0.00677	2299.97
11	540.0	16.2	3415.0	489.81	12.15	3320.26
12	450.0	1.6	3314.0	412.18	1.20	3287.31
13	275.0	16.2	1210.0	263.93	12.15	1153.16
14	45.0	1.6	185.0	44.51	1.20	187.42
Extractions (%)						
x		20.0			23.70	
y		10.0			6.52	
z		15.0			20.00	
Efficiency (%)		**52.7**			**56.4**	
Mass flow rate (kg/s)		1030			1030	
Thermal power (MW)		**1200**			**1197.3**	

6. Conclusions

The purpose of the present work is to apply an innovative optimization technique to power thermodynamic cycles proposed to run future Supercritical Water Reactors. The proposed methodology is based on coupled calculations implemented around genetic algorithms and a series of thermodynamic plant models. To this aim, the in house optimization software "BEST" is linked to a Matlab plant simulator via a DDE protocol. The simulations are performed by randomly changing key thermodynamic variables while the optimizer evaluates competing objectives until the whole process converge toward a convenient Pareto's front. A metric is introduced to control the entire iterative procedure.

This work permits us to demonstrate that the proposed cycles given in the open literature still have plenty of possibilities for increasing both efficiency and output power. In some cases, we are able to determine that the landscape of Pareto's front is mostly controlled only by few key parameters. These results may be very useful for future plant design engineers. However, it must be pointed out that none of the analyses presented in this paper are completely useful without considering essential design features, in particular for the turbines (i.e., limitations on both local pressures and amount of extracted steam, internal irreversibilities, etc.). Therefore, to include particular restrictions imposed by real turbine operation conditions, additional work should be still carried out.

Acknowledgements

This work is funded by the Natural Sciences and Engineering Research Council of Canada (NSERC) discovery grant RGPIN 41929 and the Hydro-Québec Chair in Nuclear Engineering.

References

1. International Energy Agency, "World Energy Outlook 2008," (2008).
2. Abram, T. and S. Ion, "Generation-IV Nuclear Power: A Review of the State of the Science," Energy Policy, Vol. 36, pp. 4323-4330, (2008).
3. Duffey, R., Pioro, I., Zhou, T., Zirn, U., Kuran, S., Khartabil, H. and M. Naidin, "Supercritical Water-Cooled Nuclear Reactors (SCWRs): Current and Future Concepts - Steam Cycle Options," 16th Int. Conf. Nucl. Eng., Orlando, Florida, USA, (2008).
4. Pioro, I. and R. B. Duffey, "Heat Transfer and Hydraulic Resistance at Supercritical Pressures in Power-Engineering Applications," New York, ASME Press, (2007).
5. Naidin, M., Mokry, S., Baig, F., Gospodinov, Y., Zirn, U., Pioro, I. and G. Naterer, "Thermal-Design Options for Pressure-Channel SCWRS with Cogeneration of Hydrogen," Journal of Engineering for Gas Turbines and Power, Vol. 131, pp. 012901-8, (2009).
6. Hounkonnou, W., Dipama, J., Aubé, F. and A. Teyssedou, "Multi-Objective Optimization of Thermodynamic Power Cycles Using an Evolutionary Algorithm," CNS/CAN Annual Conf., Toronto, (2008).
7. Dipama, J., Hounkonnou, W., Teyssedou, A. and F. Aubé, "A Simulation-Based Optimization of the Secondary Loop of Gentilly-2 Nuclear Power Plant," CNS/CAN Annual Int. Conf., Calgary, (2009).
8. Dipama, J., Teyssedou, A., Aubé, F. and L. Lizon-A-Lugrin "A Grid Based Multi-Objective Evolutionary Algorithm for the Optimization of Energy Systems," App. Thermal Eng., 30, pp. 807-816, (2010).
9. Dipama, J., Aubé, F. and A. Teyssedou, « Optimisation multi-objectif d'un système de cogénération à l'aide de l'algorithme évolutif BEST », VIII^{ème} Colloque Interuniversitaire Franco-québécois sur la Thermique des Systèmes, Montréal, (2007).
10. Veldhuizen, D. and G. B. Lamont, "Multi-Objective Evolutionary Algorithms: Analyzing the State-of-the-Art," Evolutionary Computation, 8 (2), pp. 125-147, (2000).
11. Goldberg, D.E. and J. Richardson, "Genetic Algorithms with Sharing for Multimodal Function Optimization," Proc. Second Int. Conf. Genetic Algorithms and their Applications, pp. 41–49, (1987).

12. Dipama, J., Teyssedou, A. and M. Sorin, “Synthesis of Heat Exchanger Networks Using Genetic Algorithms,” App. Thermal Eng., 28, pp. 1763–1773, (2008).
13. Goldberg, D.E., “Genetic Algorithms in Search, Optimization, and Machine Learning, Reading,” Addison-Wesley, 412 p., (1989).
14. Herrera, F., Lozano, M. and J.L. Verdegay, “Tackling Real-Coded Genetic Algorithms: Operators and Tools for Behavioral Analysis,” Artificial Intelligence Review, 12 (4), pp. 265-319, (1998).
15. Teyssedou, A., Dipama, J., Hounkonnou, W. and F. Aubé; “Modeling and Optimization of a Nuclear Power Plant Secondary Loop,” Nucl. Eng. Design, doi: 10.1016/j.nucengdes.2010.01.019, (2010).
16. MATHWORKS, “Matlab Operation Manual,” (2008).
17. Holmgren, M., “X Steam for Matlab,” (2006).
18. Kretzschmar H.-J. and W. Wagner, “International Steam Tables: Properties of Water and Steam Based on the Industrial Formulation IAPWS-IF97,” Second Edition, B., Springer-Verlag, Berlin, (2008).
19. Schmidt, E., “Properties of Water and Steam in SI-Units,” Springer-Verlag, Berlin, Third Edition, (1982).
20. Leyzerovich, A.S., “Steam Turbines for Modern Fossil-Fuel Power Plants,” Fairmont Press, Inc., (2008).
21. Leyzerovich, A.S., “Large Power Steam Turbines: Design and Operation,” Vol. 2. Tulsa, Oklahoma, Penn. Well Books, (1997).
22. Drbal, L.F., Boston, P.G., Westra, K.L. and B. Veatch, “Power Plant Engineering,” New York, NY, USA, Springer Science - Business Media, (1996).